UNIVERSITY OF CALIFORNIA, BERKELEY

Miyuki Weldon

E 150 Basic Modeling and Simulation Tools for Industrial Research Applications

Instructor: Tarek Zohdi

Submission Date: October 24, 2019

Modeling and Simulation of Robotic 3D Printers

1 Introduction

Modern manufacturing technology allows engineers to design and create structures of unique geometries. These methods are called additive manufacturing or 3D printing. As 3D printed products have improved in their quality and material properties, the ability to simulate them becomes more necessary. This report will explore how to model and simulate a free form, robotic 3D printer. The type of printer examined here has an extruder located on the end of a three link robot arm. Not only will the dynamics of the 3D printed material be constructed, but also of generalized robot linkages. This 3D printer will have a charged print bed, creating additional electrical attraction forces along with the drag forces. The custom material will be modeled as droplets whose properties will be determined by their base materials. The model will calculate the location of the droplets on the print bed and the particular pattern they formed. The design parameters will be optimized using a genetic algorithm to produce a desired pattern. The ability to model and simulate 3D printers will aid manufacturing technologies in producing the desired part without print failures.

2 Background and Theory

Robot Linkage Dynamics

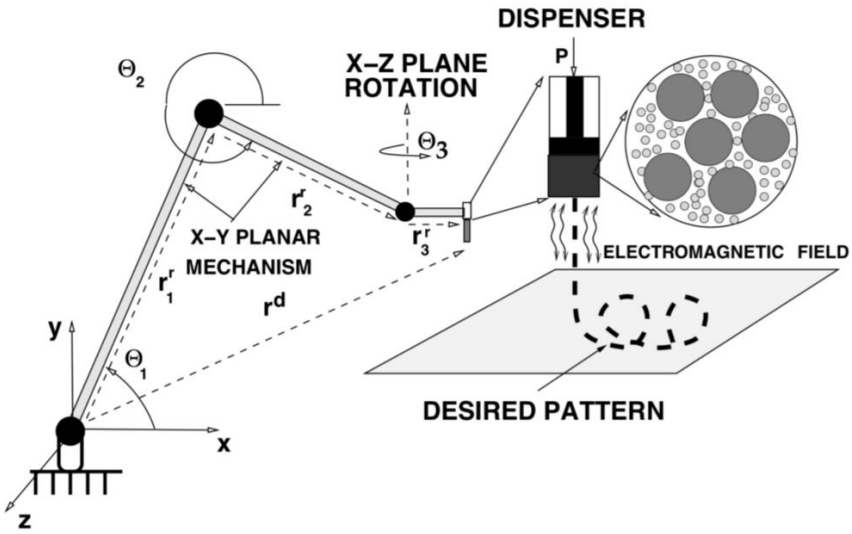

Figure 1: 3D Printer Schematic

Robots can frequently be modeled with linkages, where each link can be simplified to a vector whose magnitude is the link's length and direction is determined by the plane the link moves in and its angle from a predetermined zero. From Figure 1 we see that Link 1 and Link 2, represented by $\mathbf{r}_1^r$ and $\mathbf{r}_2^r$, respectively, move in the x-y or $\mathbf{e}_1 - \mathbf{e}_2$ plane. Similarly Link 3 ($\mathbf{r}_3^r$) is in the x-z or $\mathbf{e}_1 - \mathbf{e}_3$ plane. Using the angles noted in Figure 1 we find:

$$\mathbf{r}_1^r = L_1 cos(\theta_1)\mathbf{e}_1 + L_1 sin(\theta_1)\mathbf{e}_2$$

$$\mathbf{r}_2^r = L_2 cos(\theta_2)\mathbf{e}_1 + L_2 sin(\theta_2)\mathbf{e}_2$$

$$\mathbf{r}_3^r = L_3 sin(\theta_3)\mathbf{e}_1 + L_3 cos(\theta_3)\mathbf{e}_3$$

Knowing the short displacement from the end of the three linkages to the dispenser nozzle $\mathbf{r}_0 = -r_0\mathbf{e}_2$ we can find the dispenser location $\mathbf{r}^d = \mathbf{r}_0 + \mathbf{r}_1^r + \mathbf{r}_2^r + \mathbf{r}_3^r$.

The velocities of the linkages can be found by taking the time derivatives:

$$\dot{\mathbf{r}}_1^r = -L_1\dot{\theta_1}sin(\theta_1)\mathbf{e}_1 + L_1\dot{\theta_1}cos(\theta_1)\mathbf{e}_2$$

$$\dot{\mathbf{r}}_2^r = -L_2\dot{\theta_2}sin(\theta_2)\mathbf{e}_1 + L_2\dot{\theta_2}cos(\theta_2)\mathbf{e}_2$$

$$\dot{\mathbf{r}}_3^r = L_3\dot{\theta_3}cos(\theta_3)\mathbf{e}_1 - L_3\dot{\theta_3}sin(\theta_3)\mathbf{e}_3$$

We can find the velocity of the dispenser $\mathbf{v}^d = \dot{\mathbf{r}}^d = \dot{\mathbf{r}}_1^r + \dot{\mathbf{r}}_2^r + \dot{\mathbf{r}}_3^r$.

Our printer is simulated to have constant angular velocities $\dot{\theta_1}, \dot{\theta_2}, \dot{\theta_3}$ and known initial angles $\theta_1^0, \theta_2^0, \theta_3^0$ we can find each angle at every point in time with

$$\theta_j = \theta_j(t) = \theta_j^0 + \dot{\theta_j}t$$

As each droplet is extruded from the nozzle, its initial position in the air $\mathbf{r}_i^0$ will be determined by the dispenser's location at the time. Similarly, the initial velocity of each droplet $\mathbf{v}_i^0$ can be found with the dispenser's velocity and the relative velocity $\Delta\mathbf{v}^d$ of the extruder pushing the droplet out of the nozzle.

$$\mathbf{r}_i^0 = \mathbf{r}^d \qquad \mathbf{v}_i^0 = \mathbf{v}^d + \Delta\mathbf{v}^d$$

Droplet Dynamics

Once extruded from the nozzle, the droplet is unaffected by the robotic arm and Newton's second law ($\mathbf{F} = m\mathbf{a}$) comes into play in order to find what location each droplet will land in. Accounting for all of the forces we use:

$$m_i\ddot{\mathbf{r}}_i = \mathbf{\Psi}_i^{tot} = \mathbf{F}_i^{grav} + \mathbf{F}_i^{elec} + \mathbf{F}_i^{drag}$$

In our coordinate system $\mathbf{F}_i^{grav} = -m_i g\mathbf{e}_2$ where g is the gravitational acceleration 9.81m/s.

Because the print bed is charged, it will create an attraction force, drawing the droplets towards it. The bed is made up N_c point charges with charge q_p and fixed position $\mathbf{r}_p$.

Using the electric field, we can find the electric force of one droplet's attraction to the N_c point charges with

$$\mathbf{F}_i^{elec} = \sum_{p=1}^{N_c} \frac{q_p q_i}{4\pi\epsilon \|\mathbf{r}_i - \mathbf{r}_p\|^2}(\mathbf{r}_i - \mathbf{r}_p)$$

.

Additionally, as the droplet flies through the air, it will experience a drag force affecting its motion. Before we can calculate $\mathbf{F}_i^{drag}$ we must first find the Reynolds number Re which can be then used to find the drag coefficient $C_{Di} = f(Re)$ with a piecewise function. We can find Re and subsequently $\mathbf{F}_i^{drag}$ using

$$Re = \frac{2R\rho_a \|\mathbf{v}^f - \mathbf{v}_i\|}{\mu_f}$$

$$\mathbf{F}_i^{drag} = \frac{1}{2}\rho_a C_{Di} \|\mathbf{v}^f - \mathbf{v}_i\|(\mathbf{v}^f - \mathbf{v}_i) A_i^D$$

where $\mathbf{v}^f$ is fluid velocity, μ_f is fluid viscosity, and $A_i^D = \pi R^2$ is the drag reference area.

Droplet Material Properties

As seen in Figure 1, the custom material extruded is a combination of two well defined materials. To calculate the dynamics, it is necessary to know material properties like mass m_i and charge q_i, but the properties are not always so well defined. For properties like charge and density, the effective properties ρ^*, q^* can be found using each material's volume fractions v_2, $v_1 = 1 - v_2$ as well as the densities ρ_1, ρ_2 and charge capacity $\langle q_1 \rangle, \langle q_2 \rangle$:

$$\rho^* = (1 - v_2)\rho_1 + v_2\rho_2 \qquad q^* = (1 - v_2)\langle q_1 \rangle + v_2 \langle q_2 \rangle$$

Forward Euler Integration

After calculating all the forces on each droplet, the differential equation will be integrated for update the position and velocity for the next time step

$$\mathbf{v}_i(t + \Delta t) = \mathbf{v}_i(t) + \frac{\Delta t}{m_i}\mathbf{\Psi}_i^{tot}(t) \qquad \mathbf{r}_i(t + \Delta t) = \mathbf{r}_i(t) + \Delta t \mathbf{v}_i(t)$$

This will repeat until the droplets are on the print bed and the pattern is determined.

Simplified Dynamics

Part of this project will look at simplified dynamics, extracting away the electrical and drag forces, leaving only the gravitational force. With a constant acceleration, time stepping is not needed, and the location the droplet lands on the print bed can be solved analytically.

To find this location we start with our governing equation:

$$m_i \ddot{\mathbf{r}}_i = \mathbf{\Psi}_i^{tot} = \mathbf{F}_i^{grav} = -m_i g \mathbf{e}_2$$

This gives us the constant acceleration $\ddot{\mathbf{r}}_i = -g\mathbf{e}_2$. From there we can integrate to find the velocity and position.

$$\mathbf{v}_i = \int_0^t \ddot{\mathbf{r}}_i dt = \ddot{\mathbf{r}}_i t + \mathbf{v}_i^0$$

$$\mathbf{r}_i = \int_0^t \mathbf{v}_i dt = \frac{1}{2}\ddot{\mathbf{r}}_i t^2 + \mathbf{v}_i^0 t + \mathbf{r}_i^0$$

We want to know the droplet's position when it lands on the print bed. To do this we need the vertical position (in the $\mathbf{e}_2$ direction) of the droplet

$$\mathbf{r}_i \cdot \mathbf{e}_2 = -\frac{1}{2} g t^2 + v_{i2}^0 t + r_{i2}^0$$

We can use this equation to find landing time when $\mathbf{r}_i \cdot \mathbf{e}_2 = 0$

$$t_{land} = \frac{-v_{i2}^0 \pm \sqrt{(v_{i2}^0)^2 - 4(-\frac{1}{2}g) r_{i2}^0}}{-g}$$

and take the physically valid solution. We can find the $\mathbf{e}_1$ and $\mathbf{e}_3$ coordinate with

$$\mathbf{r}_i(t_{land}) \cdot \mathbf{e}_1 = v_{i1}^0 t_{land} + r_{i2}^0$$

$$\mathbf{r}_i(t_{land}) \cdot \mathbf{e}_3 = v_{i3}^0 t_{land} + r_{i3}^0$$

giving us our position on the build plate.

3 Procedure and Methods

The procedure was split into two sections: **Part 1**, modeling the droplet dynamics with gravitational, drag, and electrical forces for one pattern given by predefined angular velocities and extrusion velocity and **Part 2**, removing the drag and electrical forces to simplify the model and improve run time in order to optimize the pattern using a genetic algorithm

In Part 1, to improve code run time, I was able to calculate the dispenser locations at every point in time for a time step of Δt up to a total T seconds. This was all done with vector operations and no loops because the angles for every time step could be calculated. Because the printer was known to release a droplet at every time step, these locations could be translated to the initial locations for each droplet. The time that the droplet left the extruder is not important because of the assumption that the droplets will not interact with each other. Inside a time loop, all of the forces were calculated using vector operations. The electrical force required each droplet (with $\mathbf{e}_1, \mathbf{e}_2, \mathbf{e}_3$ coordinates) to interact with all N_c^2 point charges (also with $\mathbf{e}_1, \mathbf{e}_2, \mathbf{e}_3$ coordinates) so it was calculated using two 2-dimensional matrices (a $3 \times N_t \times 1$ and a $3 \times 1 \times N_c$) that were perpendicular to each other. These matrices were subtracted to create a 3-dimensional matrix ($3 \times N_t \times N_c$). This matrix was then used to do vector operations on and eventually summed along the third dimension to calculate $\mathbf{F}_i^{elec}$. A flag array of trues where the droplet had not landed and falses when it had was used to only continue updating the locations of droplets that had not landed. It was updated and the landing time was stored using only vector operations resulting in quick code.

In Part 2, the electrical and drag forces were stripped away allowing me to remove the time loop because the drop locations on the bed could be calculated analytically with the constant acceleration of gravity. The design variables $\mathbf{\Lambda} = \{\dot{\theta}_1, \dot{\theta}_2, \dot{\theta}_3, \Delta \mathbf{v}^d\}$ are varied to generate different patterns $\mathbf{r}_i^{gen}$. A genetic algorithm optimizes them to construct a desired

pattern $\mathbf{r}_i^{des}$. The GA minimizes the cost function:

$$\Pi = \frac{\sum_{i=1}^{N_d} \|\mathbf{r}_i^{des} - \mathbf{r}_i^{gen}\|}{\sum_{i=1}^{N_d+1} \|\mathbf{r}_i^{des} - \mathbf{r}_{i+1}^{des}\|}$$

While this cost function decreases as the patterns get more similar, its value and any threshold are relative to how it is scaled. The denominator term is the arc length of the desired pattern and scales the cost function to allow patterns that are similar in shape but not in size to have a good score. Additionally it nondimensionalizes the cost function. However, this is not a unique nor necessarily optimized cost function. As we will see later, it is likely not the best cost function.

4 Results and Discussion

Part 1: Full Model with Electrical and Drag Forces

Using the given values of $\dot{\theta}_1 = 0.2rad/s, \dot{\theta}_2 = -0.2rad/s, \dot{\theta}_3 = 10rad/s, \Delta\mathbf{v}^d = -1.2\mathbf{e}_2$, I was able to generate a pattern with all forces.

As seen in Figure 2a, the pattern produced is a nice spiral pattern. From the given constant angular velocities and the known length of time T = 3sec, we can see that Links 1 and 2 will only rotate approximately 34 degrees in that 3 seconds; however, Link 3 will complete 6.6 revolutions. This demonstrates that most of the pattern shape variation will come from the motion of Link 3 which is spinning around in a plane parallel to the print bed. The other two links are moving much slower and in opposite directions moving the connection point of Link 3 in the $-\mathbf{e}_1$ and $-\mathbf{e}_2$ direction. This is adjusting the center of the circle Link 3 is drawing, resulting in the spiraling effect.

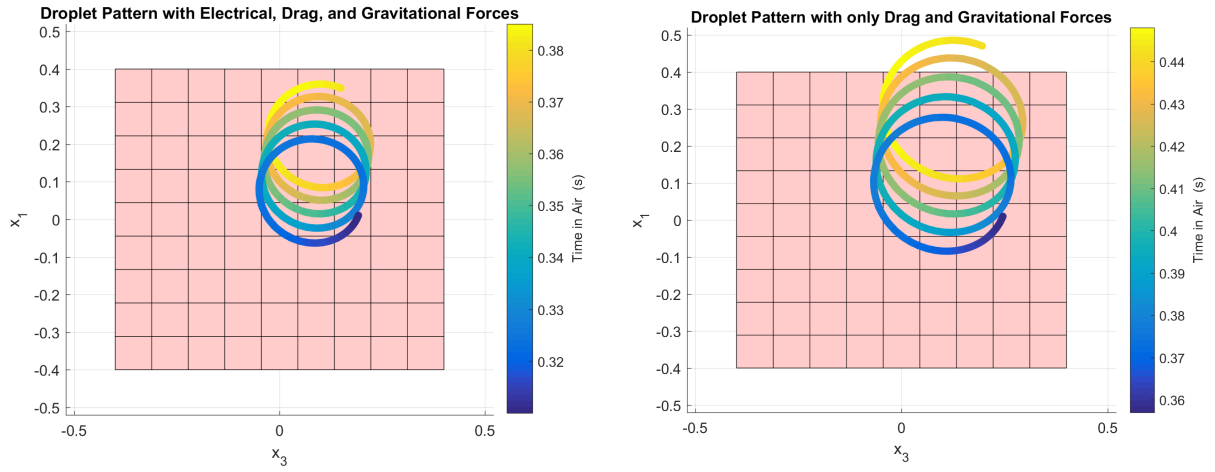

(a) With Full Forces

(b) Without Electrical Forces

Figure 2: Top-Down Final Droplet Pattern

As we can see, the electrical force keeps the print on the print bed (represented by the light red surface). Because all of the evenly spaced point charges are "on" all the time, the electrical force will draw the droplets towards the center of the print bed. Because the

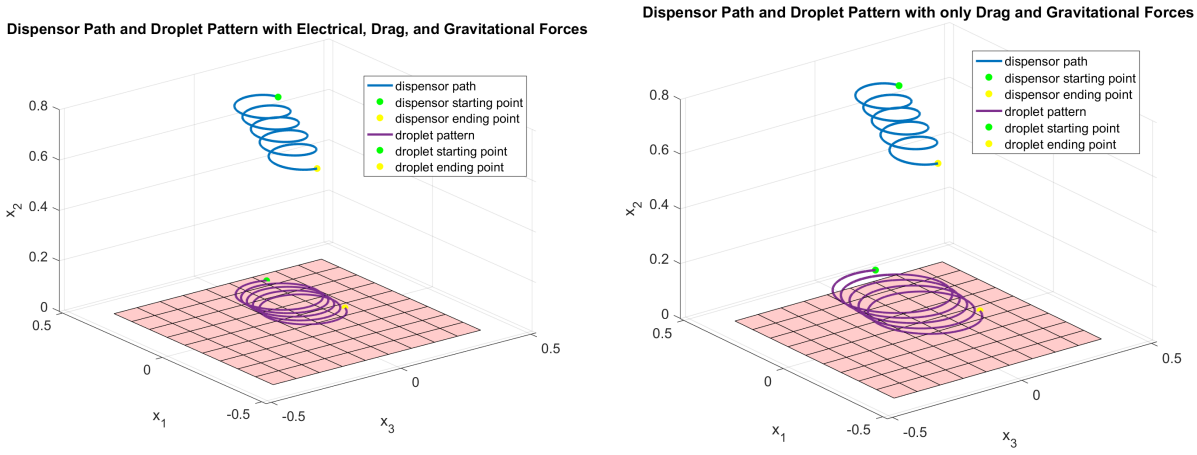

(a) With Full Forces

(b) Without Electrical Forces

Figure 3: Robot Arm Path and Final Droplet Pattern

links can rotate at high speeds, the initial velocity of the droplet when it is extruded from the dispenser can have a direction pointing off to the side of the print bed. The electrical forces prevent these "flinging" droplets from landing anywhere outside of the print bed. If only some point charges were "on," the electrical force could influence it into a certain shape.

Part 2: Simplified Model without Electrical and Drag Forces for Genetic Algorithm

For the genetic algorithm, 100 design strings ($\mathbf{\Lambda}$) are randomly generated within predetermined bounds for all of the design parameters. These parameters are plugged into the cost function which generates a pattern $\mathbf{r}_{gen}$ and measures it against the desired pattern $\mathbf{r}_{gen}$ then gives it a score of how close it is determined by the function $\Pi(\mathbf{\Lambda})$ described in the last section. The scores are ranked and the top 10 parents create 10 offspring which are weighted combinations of the parents. The remaining design strings are removed and 80 more are randomly generated. That process completes a generation. This repeats until the cost of the best design is below a tolerance $Tol = 2 \times 10^{-2}$ or it reaches the maximum number of generations G = 100.

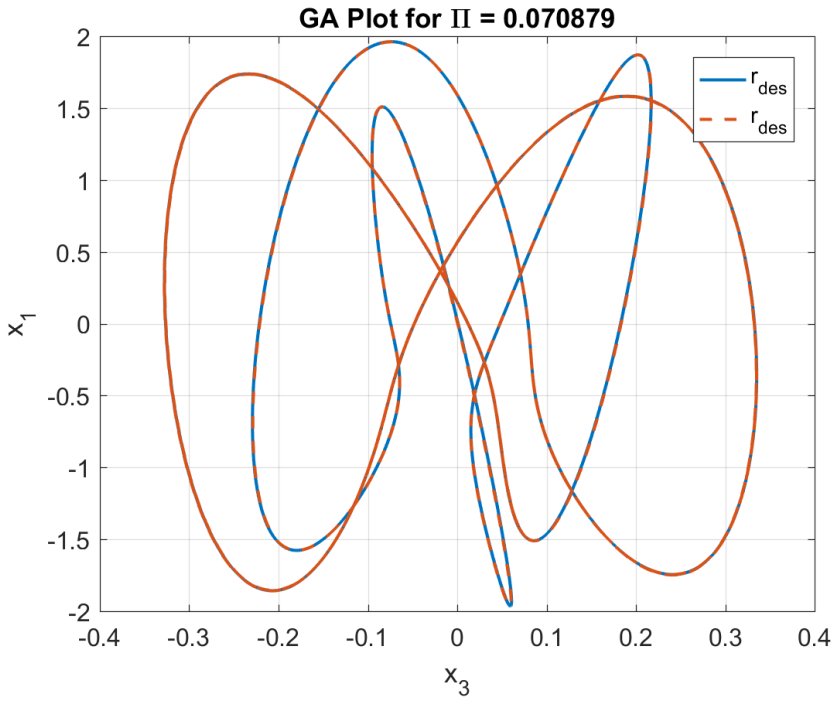

Figure 4: Pattern Generated by the Best Cost Design

Although running quickly, my cost was never able to fall below the tolerance. However, it could reach a tolerance of $Tol = 1 \times 10^{-1}$. As we can see in Figure 4, the pattern matches the desired pattern quite closely, and that is reflected in the cost $\Pi(\mathbf{\Lambda_1}) = 0.070879$. My code's inability to reach the original tolerance can be attributed to the choice of cost function. The arc length in the denominator acts as a scaling factor and will affect the cost function's ability to fall below the tolerance.

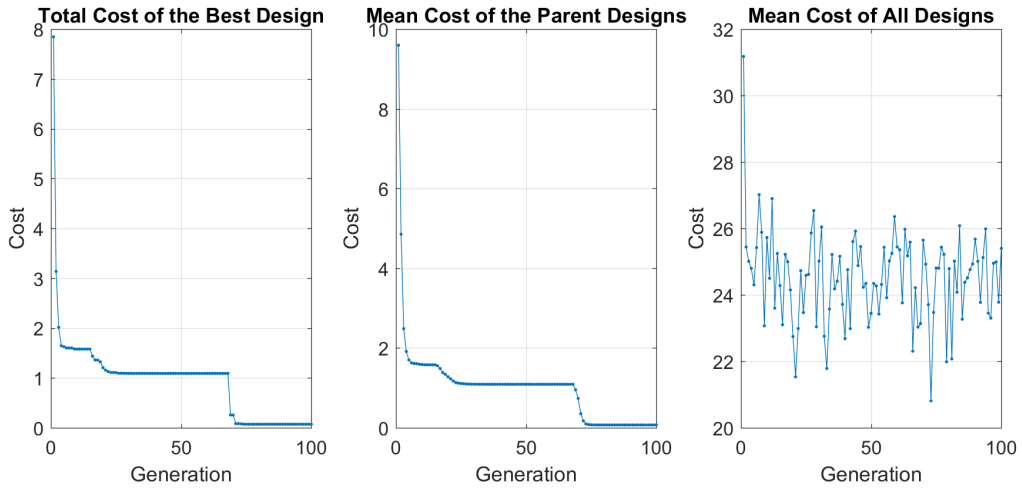

Figure 5: Convergence Plots for the Total Cost

We can see from the convergence plots in Figure 5 that the GA runs for the full 100 generations because it never reaches that initial tolerance, and then plateaus. Another possible reason for the difficulty in reaching the tolerance could be because the cost function has lots of little peaks, making it hard for the offspring of the parents to improve their scores. In that case, the ability to reach a point below that threshold would be up to chance when the design strings are all randomly generated, making it unlikely to reach that tolerance.

Additionally, as seen in Table 1, it is not surprising that all four design vectors have the same values because the desired pattern will have a unique set of parameters to recreate it.

Table 1: Best Performing $\mathbf{\Lambda}$ Designs

	$\dot{\theta}_1$	$\dot{\theta}_2$	$\dot{\theta}_3$	$\Delta \mathbf{v}^d$
1	15.7085	15.7093	6.2827	-3.1468
2	15.7085	15.7093	6.2827	-3.1468
3	15.7085	15.7093	6.2827	-3.1468
4	15.7085	15.7093	6.2827	-3.1468

5 Conclusion

In this report, we have seen that a free form robotic 3D printer can be modeled with complex dynamics and optimized with simple dynamics. While the combination of the two is possible, it will require a lot of patience, a faster coding language, a more efficient machine learning algorithm, or all of the above. Despite this, we have constructed a basis for calculating the optimal settings of a free form printer to produce a specified geometry. The most important aspect of a 3D printer, or any manufacturing process, is turning a design into a physical part accurately and precisely within the manufacturing tolerance. This type of modeling is necessary for any 3D printer to be useful. One part of this model that has been abstracted away is the material behavior. Each droplet's adhesion on the print bed and with each other as well as its deformation upon contact are critical factors in determining the final geometry of the part. These factors require knowledge of effective material properties which can be more complex to calculate for certain properties. Another complexity could be a robot with non-constant angular velocities. Calculating the end effector path would be much more complicated and could involve advanced robot kinematics. As we have seen, free form 3D printers are not limited to this situation, but this model provides a necessary framework for creating more accurate simulations of physical systems.